



Aggregation-Induced Fluorescence of Carbazole and *o*-Carborane Based Organic Fluorophore

Jiemin Jiao¹, Jia-Xin Kang¹, Yanna Ma¹, Qianyi Zhao¹, Huizhen Li¹, Jie Zhang¹ and Xuenian Chen^{1,2*}

¹ School of Chemistry and Chemical Engineering, Henan Key Laboratory of Boron Chemistry and Advanced Energy Materials, Henan Normal University, Xixiang, China, ² College of Chemistry and Molecular Engineering, Zhengzhou University, Zhengzhou, China

Carbazole based fluorophores 9-butyl-3,6-bis-(phenylethynyl)-9H-carbazole (1) and 9-butyl-3,6-bis-(2-phenyl-*o*-carborane)-9H-carbazole (2) were synthesized *via* Sonogashira type cross-coupling reaction and followed by insertion with decaborane. Compound 1 exhibited far more intense fluorescence than 2 in THF solution, while in solid state 2 exerted stronger fluorescence than 1. The fluorescence quenching behavior of 2 in THF solution could be attributed to the intramolecular charge transfer of donor-acceptor system in 2, which was confirmed by electrochemical experiments and DFT calculations. The fluorescence enhancement of 2 in solid state can be ascribed to aggregational induced packing which was evidenced by crystallographic study. In addition, compound 2 showed typical aggregation induced emission (AIE) behavior.

OPEN ACCESS

Edited by:

Guigen Li,
Texas Tech University, United States

Reviewed by:

Cheng Yixiang,
Nanjing University, China
John M. Rimoldi,
University of Mississippi, United States

*Correspondence:

Xuenian Chen
xnchen@htu.edu.cn

Specialty section:

This article was submitted to
Organic Chemistry,
a section of the journal
Frontiers in Chemistry

Received: 24 June 2019

Accepted: 24 October 2019

Published: 15 November 2019

Citation:

Jiao J, Kang J-X, Ma Y, Zhao Q, Li H,
Zhang J and Chen X (2019)
Aggregation-Induced Fluorescence of
Carbazole and *o*-Carborane Based
Organic Fluorophore.
Front. Chem. 7:768.
doi: 10.3389/fchem.2019.00768

Keywords: carbazole, carborane, fluorescence, AIE, donor-acceptor system

INTRODUCTION

Organic π -conjugated compounds have attracted much attention in the realm of functional material science for over a few decades because of their intrinsic flexibility on structural designing and functional modifying, as well as low cost and sustainable manufacturing potential in contrast to metal (especially rare-earth metal) based materials (Metzger, 1999; Beverina and Pagani, 2014). Among the organic functional π -conjugated materials, push-pull type chromophores with electron donating (donor) and accepting (acceptor) functional groups are of growing interests for their promising electro-optical properties and straightforward designing strategy (Kivala and Diederich, 2009). Introducing strong donor and acceptor into π -conjugated molecule structure results in complicated photo- and electronic- behaviors, leading to the discovery of various functional materials which could be applied in the field of organic light-emitting diodes (OLED) (Grimsdale et al., 2009; Xiao et al., 2011), semiconducting materials (Zhang et al., 2017), and organic solar cells (Gunes et al., 2007; Cheng et al., 2009; Mishra and Bauerle, 2012).

Carbazole demonstrates stability toward thermal, chemical, and environmental factors, and is also known for its excellent electron donating and charge transporting properties. Meanwhile, carbazole building block is easy to be functionalized at either nitrogen or aromatic backbones. With all these advantages, carbazole has been widely used and studied in photoluminescent and electronic materials (Grazulevicius et al., 2003; Kundu et al., 2003; Grigalevicius, 2006; Blouin and Leclerc, 2008; Karpicz et al., 2010; Chen et al., 2011; Li et al., 2012; Ooyama et al., 2012; Uoyama et al., 2012; Nishimoto et al., 2014; Yang et al., 2016; Wex and Kaafarani, 2017; Meier et al., 2019). *o*-Carborane (1,2-dicarba-*closo*-dodecaborane) hosts electronic deficient property due to the uniquely delocalized 3-center-2-electron bond on its electron withdrawing icosahedron boron

cluster skeleton, and possesses highly polarized σ -aromatic character (Naito et al., 2015; Cho et al., 2016; Wu X. Y. et al., 2018). These features allow *o*-carborane cage to act as an acceptor through π -conjugated system, and the molecule exhibits interesting photoelectronic properties (Li et al., 2016; Nishino et al., 2016; Núñez et al., 2016; Naito et al., 2017). In the last few years, many works have been focused on donor-acceptor type π -conjugated compounds based on carbazole and *o*-carborane moieties due to the fore-mentioned advantages, and some of them are inspiring (Kwon et al., 2014; Furue et al., 2016). Recently, Yan's group reported a serial of carboranyl carbazoles exhibiting both aggregational induced emission (AIE) and electrochemical luminescence behavior in aqueous solution, which has strong potential for biochemical and diagnostic applications (Wei et al., 2019).

Researches on AIE have thrived since its discovery in 2001 (Luo et al., 2001), because this type of compounds exert excellent photoelectronic behaviors in condensed or solid state rather than solution, make it possible and convenient to design novel organic photoelectronic devices such as chemo- or bio-sensor, OLED, organic field-effect transistor (Hong et al., 2009, 2011; Ding et al., 2013; He et al., 2015). Herein, we report a carbazole and carborane based organic fluorophore which exhibits typical AIE behavior.

RESULTS AND DISCUSSION

Synthesis

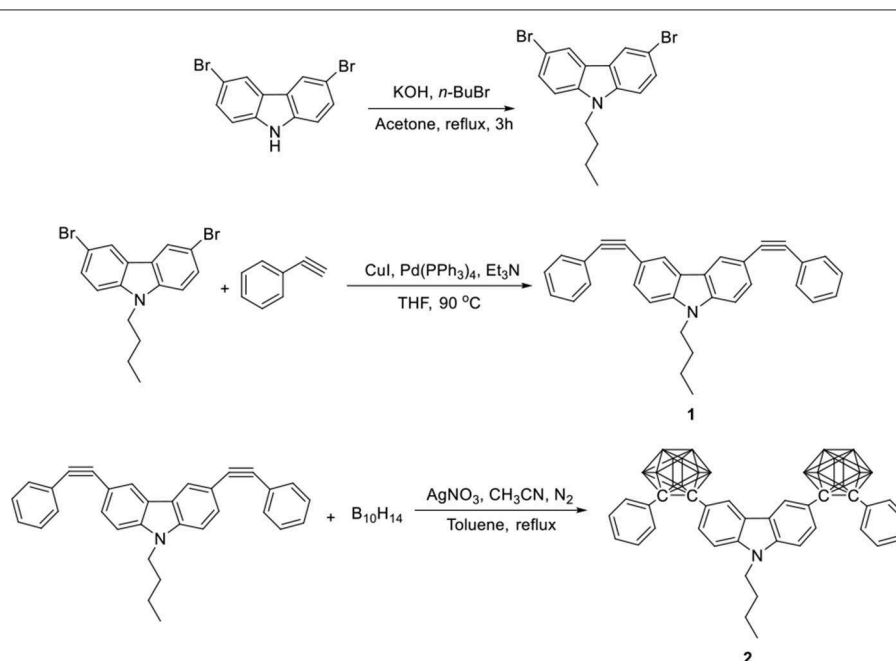
The synthetic procedures are shown in **Scheme 1**. According to the literature methods (Toppino et al., 2013; Zhu et al., 2016), 3,6-dibromo-9-butylcarbazole was *N*-alkylated in the presence

of potassium hydroxide, and then followed by Sonogashira type cross-coupling reaction with phenylacetylene to afford 9-butyl-3,6-bis-(phenylethynyl)-9H-carbazole (**1**). 9-butyl-3,6-bis-(2-phenyl-*o*-carborane)-9H-carbazole (**2**) was prepared by the insertion reaction of **1** and decaborane under a refluxing condition in toluene/CH₃CN in the presence of a catalytic amount of silver nitrate. As a new compound, **2** was characterized by NMR, IR, and X-ray crystallography (see **Figures S1–S7**, **Table S1**, and **Check CIF Report in Supplementary Material**).

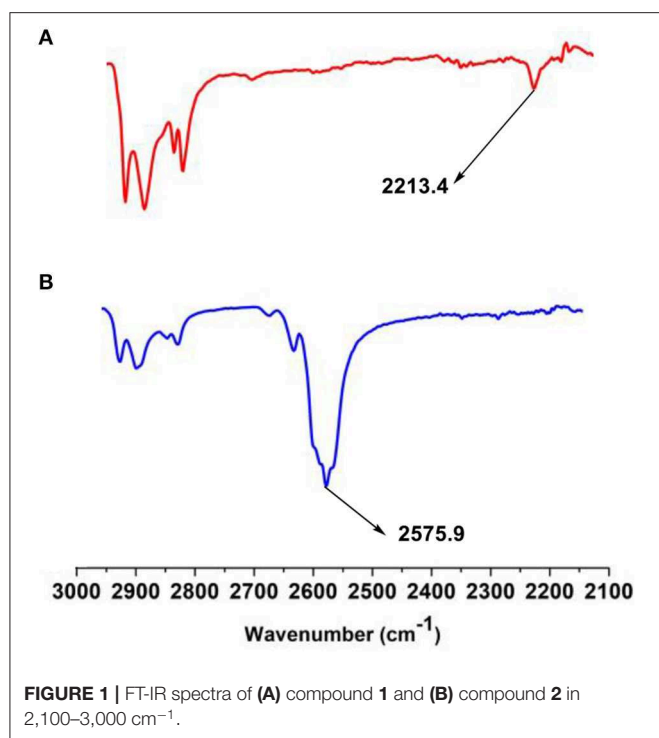
FT-IR and UV-vis Spectra

In the FT-IR spectrum of **1** (**Figure 1**), the absorption at 2,213 cm⁻¹ is considered to be the C-C triple bond absorption, which disappeared in the FT-IR spectrum of **2**, indicating the insertion reaction of decaborane and alkyne moiety of **1**. Also, the appearance of strong absorption of B-H vibration at 2,576 cm⁻¹ confirmed the existence of B-H bond in compound **2**, indicating the conversion from **1** to **2** (Yin et al., 2018).

The UV-vis absorption spectra of **1** and **2** were recorded in THF solution. As shown in **Figure 2**, the absorption band at 260, 310, and 330 nm could be assigned to the n - π and n - π^* transition of electron-enriched carbazole (Cz) moiety to the phenylacetylene fragment of **1** (Li et al., 2012; Gong et al., 2014), while blue shift was observed for the absorption band at 260 and 310 nm of compound **2**. This blue shift effect could be attributed to the wider HOMO/LUMO energy gap on Cz fragment caused by the highly electron-deficient *o*-carborane (Cb) moiety of **2** (Yokoyama et al., 2018). Moreover, the formation of Cb cluster in **2** leads to the disruption of donor-linker-acceptor conjugated system (Cz-phenylacetylene), hence the absorption band of intramolecular charge transfer transition at 330 nm is



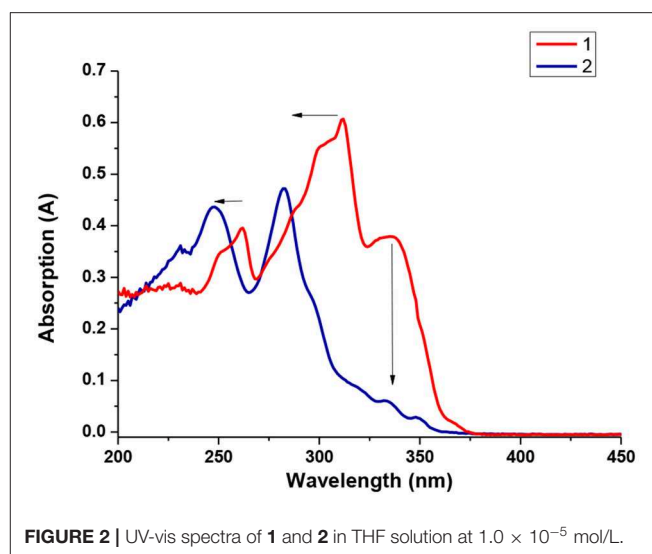
SCHEME 1 | Synthetic procedures for **1** and **2**.



highly reduced (Wang et al., 2018; Wu Q. J. et al., 2018), as evidenced in **Figure 2**.

Fluorescence Behaviors

The fluorescence spectra of compound **1** and **2** in various of solutions were recorded, and THF was chosen as solvent for the investigation of the solution excited behaviors. Upon excitation at 304 nm, compound **1** exhibits intense fluorescent emission at around 395 nm in THF solution, and the Stokes shifts, which are determined by the difference in the wavelength between position of the band maxima of the excitation and emission spectra of the same electronic transition were almost identical in different solvents (**Figure 3A** and **Figure S8**). In the case of compound **2**, significant fluorescence quenching effect was observed (**Figure 3C**). Also, in various solutions of **2** at higher concentration, the fluorescence emissions vary from 299 to 360 nm upon excitation at 255 nm (**Figure 3B** and **Figure S9**), indicating the different photoluminescence mechanism. The intense blue fluorescent emission of compound **1** can be assigned to the local excited-state emission of a Cz-phenylacetylene fragment (Li et al., 2019), and the solvatochromic shift of **2** suggested the intramolecular charge-transfer (ICT) behavior between Cb and Cz units (Wee et al., 2012a; Nghia et al., 2018b). The temperature dependency of emission of **2** was also investigated (**Figure S10**), the results showed that the fluorescence intensity of **2** slightly decreased when temperature rises, implying that the emission band at around 348 nm was from twisted-ICT state, whose emission effect could be affected by environment conditions such as polarity of solvent and temperature (Nishino et al., 2017).



Solid state fluorescence behaviors of compound **1** and **2** are also studied, detailed data are listed in **Table 1**. As shown in **Figure 4**, compound **1** exerts fluorescence at 455 nm with a shoulder peak situated at 410 nm, and compound **2** shows a relatively sharp single peak at 550 nm. For compound **1**, the major emission band at 455 nm could be assigned to the $n-\pi$ and $\pi-\pi^*$ local excited state emission of Cz-phenylacetylene fragment, and the minor shoulder emission peak at 410 nm comes from the isolated emission of Cz moiety (Li et al., 2019). Time-resolved measurement (**Figures S11, S12; Tables S2, S3**) also confirmed the bi-exponential decay behavior of **1**, indicating the double excited state. It is interesting that **2** exhibits stronger fluorescent emission than **1** in solid state, whereas in THF solution the fluorescent emission of **2** is nearly quenched completely. This phenomenon could be related to the photoluminescence mechanism for compound **1** and **2**. As we formerly discussed, in THF solution the fluorescent emission of **1** comes from the local excited-state emission of a Cz-phenylacetylene conjugated fragment, which no longer exists in **2** because of the introduction of Cb moiety (Nghia et al., 2018a). Also, the ICT quenching effect caused by the highly electron-deficient Cb inhibits the fluorescent emission of **2** (Wu Q. J. et al., 2018). Hence in THF solution, compound **1** exerts a much stronger fluorescence intensity than **2**.

X-ray Crystallographic Studies

The fluorescence enhancement of compound **2** in solid state is considered to be affected by the aggregational packing in its solid state. The X-ray crystallographic analysis of **2** indicated that two phenyl groups and one Cz unit adopted a Z-shaped arrangement. The C-C bond lengths of two Cb units are without much distinction (1.736 Å for C17-C18 and 1.733 Å for C19-C20, **Figure 5A**) due to the rigidity of Cb cluster. Nevertheless, the torsion angles around the carbon atoms of Cb explain their environmental difference in detail. The colored carbon atoms and C-C bonds in **Figure 5A** are from the Cb-phenyl units (including phenyl unit in Cz), they can also be considered as

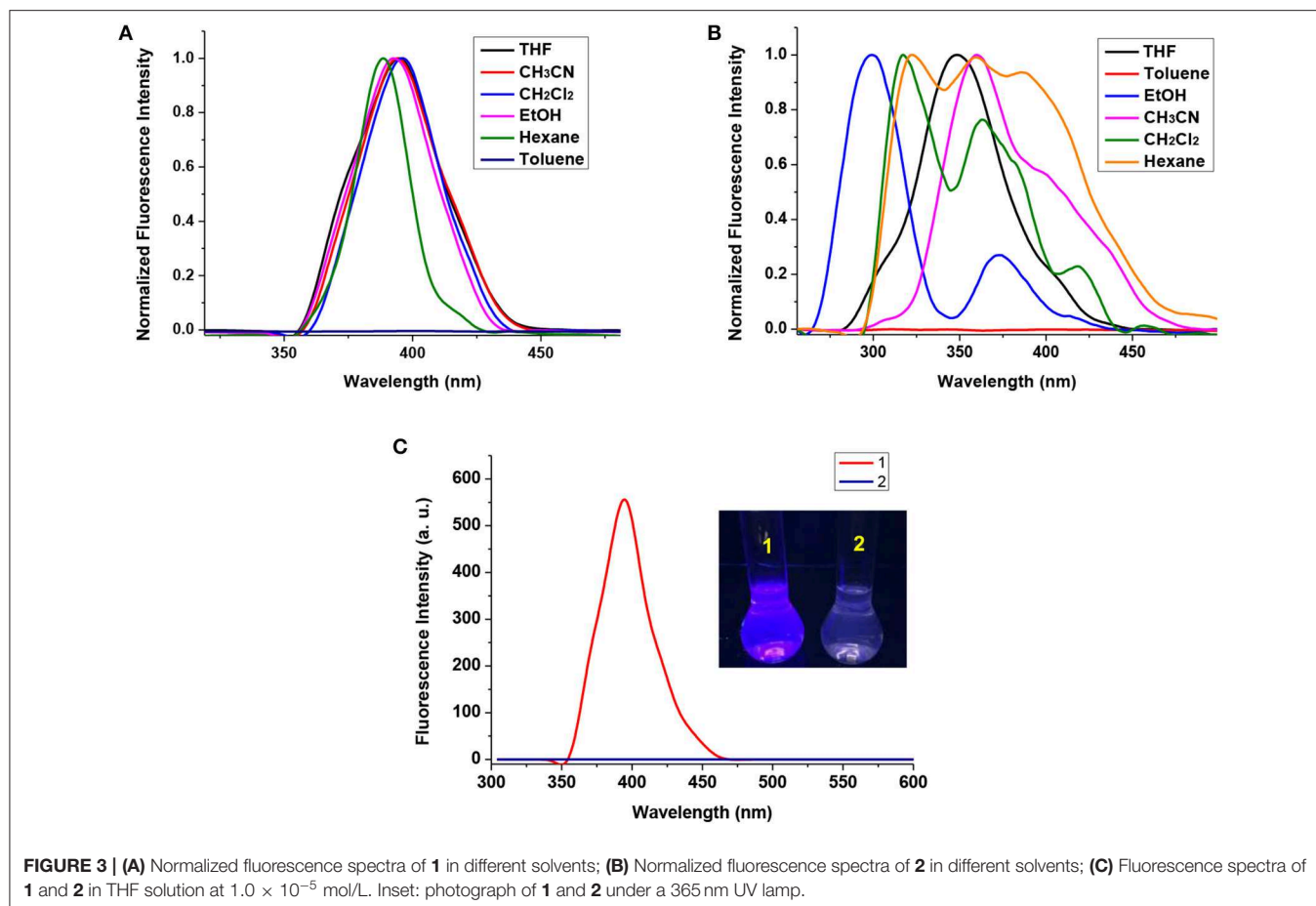


TABLE 1 | Photo-physical datas of **1** and **2**.

Compound	$\lambda_{\text{abs}}/\text{nm}^{[a]}$	$\lambda_{\text{ex}}/\text{nm}$		$\lambda_{\text{em}}/\text{nm}$		$\tau_1/\text{ns}^{[b]}$	$\tau_2/\text{ns}^{[b]}$	PLQY	
		[THF]	[solid]	[THF]	[solid]			Φ_F^c	Φ_F^d
1	260/310/330	304	399	395	462	1.52	4.18	0.34	0.15
2	247/280	255	399	348	538	5.59	—	0.03	0.56

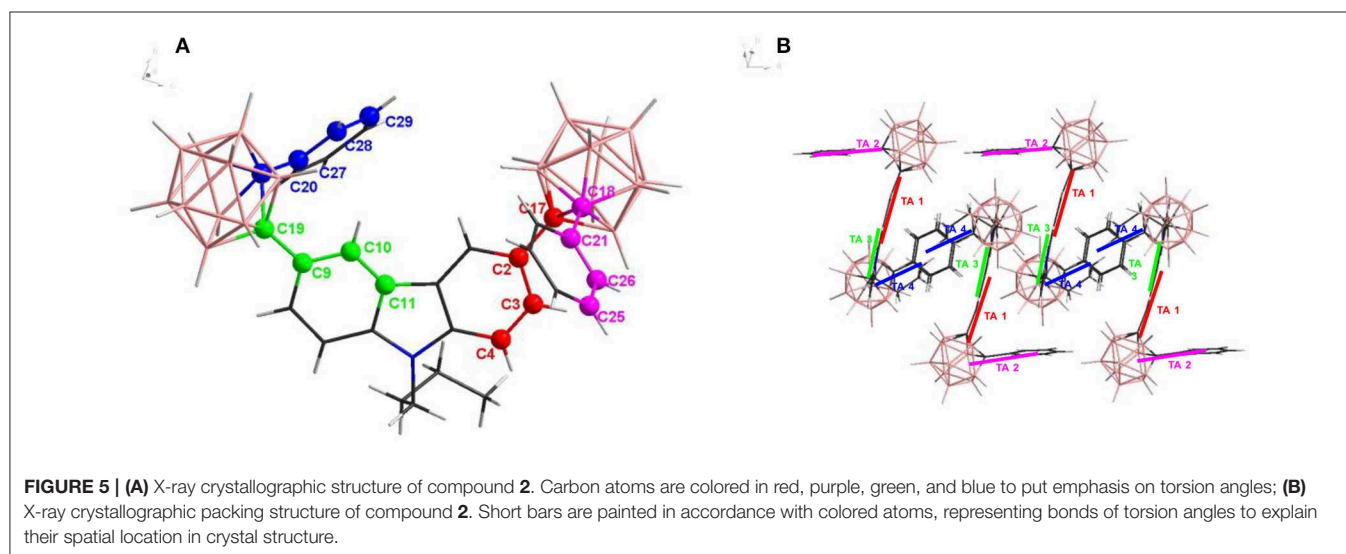
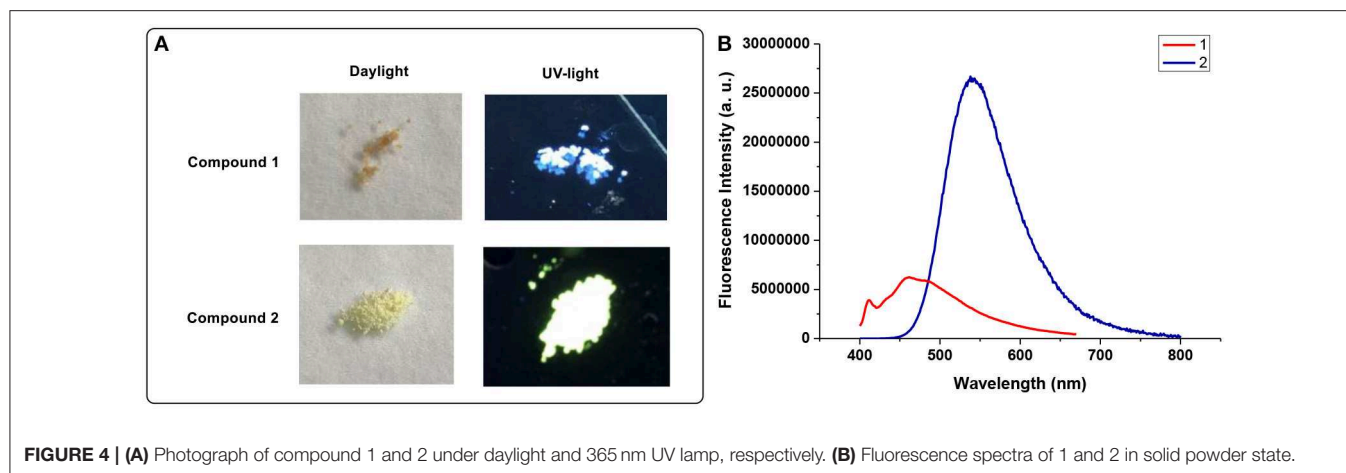
^aCollected in N_2 -saturated THF solution at 1.0×10^{-5} mol/L under room temperature. ^bCollected in solid state. Photoluminescence quantum yields taken in ^cTHF solution at 1.0×10^{-5} mol/L and ^dsolid state.

carbon atoms linked to phenyl units as well, and their torsion angles shall be 180° in a theoretically free environment without spatial hindrance. As shown in **Table 2**, the torsion angles of C17 and C18 are relatively smaller than C19 and C20, suggesting that Cb (C17-C18) is in a more distorted environment than Cb (C19-C20), which also indicates that there is a tightly packing style in solid state of compound **2** (**Figure 5B**). In THF solution of **2**, the rapid charge transfer from the fluorophore of Cz to the electron-withdrawing units of Cb weakens its fluorescent emission, while in solid state of **2**, intramolecular vibration and rotation are greatly restricted due to its tightly packing structure, which blocks the non-radiative pathway of excited state annihilation and opens up the radiative channel, thus its solid state fluorescent emission is enhanced (Zhu et al., 2008).

Moreover, the prolonged fluorescence life of **2** also confirmed this restriction effect.

AIE Studies

In order to further demonstrate the AIE behavior of compound **2**, the fluorescent emission spectra in THF/ H_2O solution with different volumetric ratios (fraction of water, or f_w in vol.%) were determined, and the results are shown in **Figure 6**. Compound **2** virtually showed weak fluorescent emission in either THF solution or THF/ H_2O solution with low H_2O volume fraction. However, its fluorescent emission was significantly enhanced when f_w reaches 70%, and the emission intensity kept increasing as the f_w rises at higher levels. When f_w reached 95%, bright yellow fluorescence could be observed



directly under commercially available UV lamp upon excitation at 254 nm. This typical AIE behavior could be ascribed to the decrease of solubility of 2 with the gradual addition of H₂O. In THF solution, the fluorescence emission comes from the ICT emission and it is weak because the ICT quenching effect of the introduced carborane unit. As water fraction increased, the emission wavelength around 538 nm originating from the lowest energy ICT excited state was significantly enhanced with the formation of aggregation, which leads to the restriction of vibration and/or rotation of Cb and phenyl unit in compound 2. In the THF solution, the Cb and phenyl unit can rotate, resulting in the dissipation of the excitation energy as thermal energy. However, when the molecules aggregated, the rotation of the peripheral carborane and phenyl units are effectively impeded, which could not lead to non-radiative decay any longer, thus the molecules of 2 become strongly emissive (Furue et al., 2016). In fact, the THF/H₂O solutions of 2 showed rather poor clarity at higher f_w level in contrast to its lower f_w solution, indicating that other than precipitation, this aggregation process was conducted at nanoscale (Liu et al., 2011).

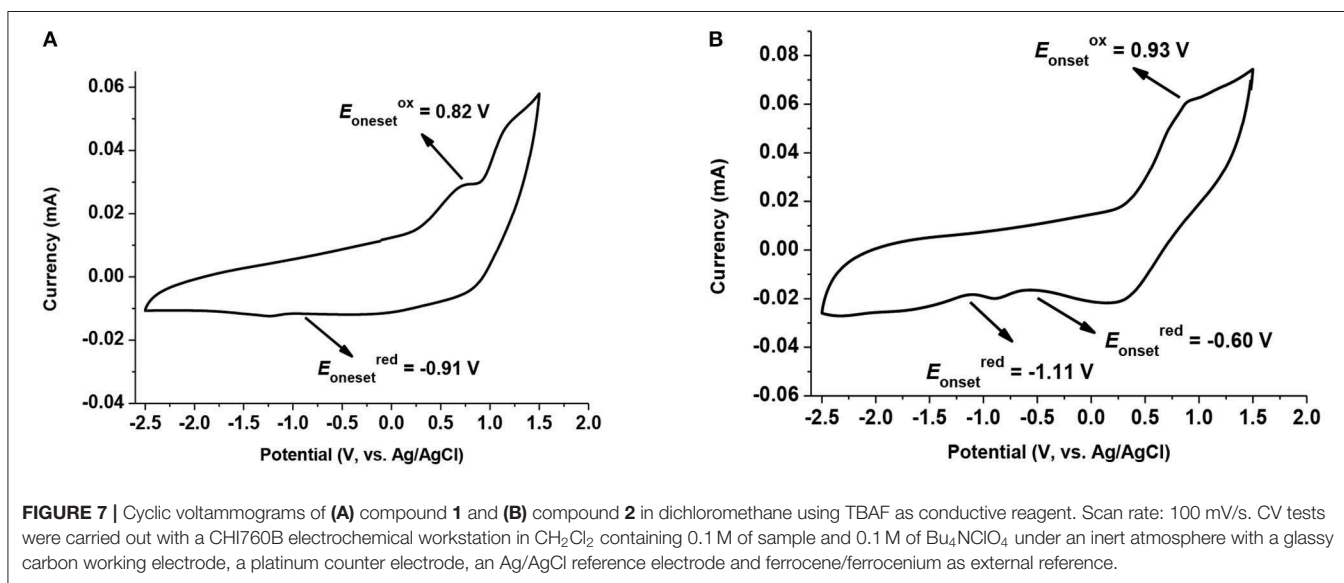
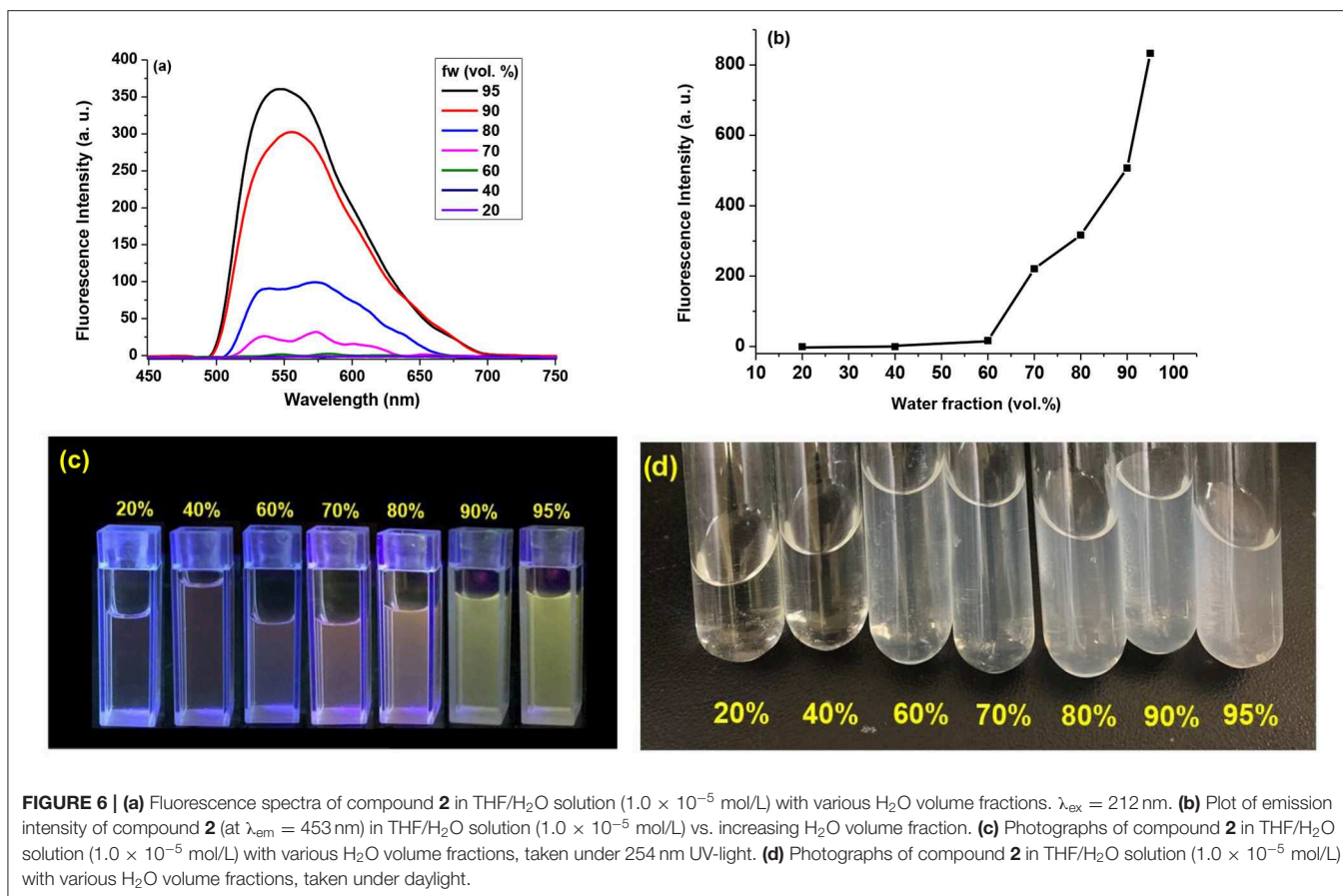
TABLE 2 | Torsion angle in compound 2.

Label	A-B-C-D	Torsion Angle (°)
TA 1	C17-C2-C3-C4	171.3
TA 2	C18-C21-C26-C25	173.4
TA 3	C19-C9-C10-C11	177.9
TA 4	C20-C27-C28-C29	176.2

TA, Torsion Angle.

Electrochemical Behavior

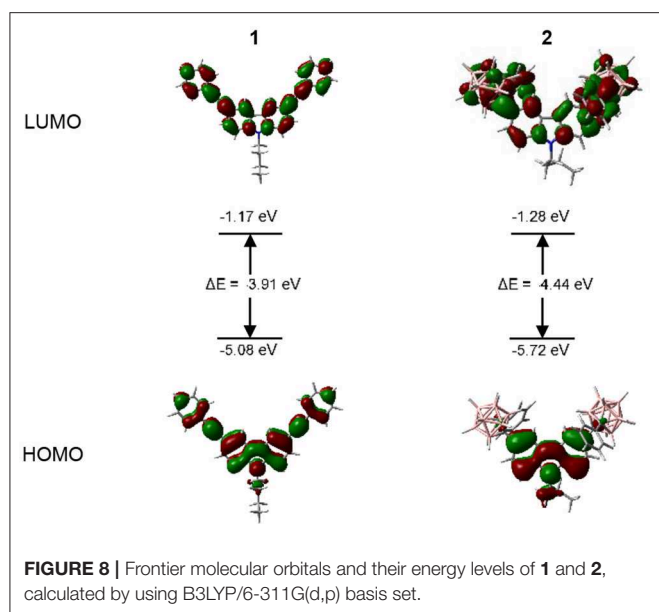
Furthermore, cyclic voltammograms (CV) were also collected for both 1 and 2 by using dichloromethane with tetrabutylammonium perchlorate (TBAF), as reported in the literature for illustration on their electrochemical properties (Hosoi et al., 2011). The CV curve of 1 (Figure 7A) shows an oxidation peak at 0.82 V and a reduction peak at -0.91 V, might be ascribed to the electrochemical redox process on nitrogen atom in Cz skeleton (Kundu et al., 2003; Naito et al., 2018). In the case of 2 (Figure 7B), one more reduction peak of Cbs was recorded at -1.11 V,



and redox peaks of Cz shifted to higher voltage (from 0.82/−0.91 to 0.93/−0.60), this is supposed to be the electron withdrawing effect of Cbs, making the oxidation process harder by dispersing the electron density on Cz skeleton, and confirming the donor-acceptor behavior in the structure of **2**.

DFT Calculation

DFT calculations were performed to determine the HOMO and LUMO energy levels of compound **1** and **2**. The Results show that the introduction of *o*-Cb units lowered both the HOMO and LUMO energy level (from −1.17 to −1.28 eV for LUMO, and from −5.08 to −5.72 eV for HOMO), this could



be attributed to the electron-withdrawing ability of the *o*-Cb groups (Kokado and Chujo, 2009; Kokado et al., 2010; Wee et al., 2012b, 2013; Guo et al., 2015; Wu X. Y. et al., 2018). From **Figure 8**, it could be noted that the HOMO and LUMO were mainly located in the Cz-phenylethynyl conjugated skeleton for **1**, which is in accordance with the local excited state fluorescence emission. As for the case of **2**, the LUMO distributed over the conjugated Cz-Cb skeleton, while its HOMO density was mainly delocalized in the Cz moiety, indicating that the conjugation was greatly reduced in contrast to **1** due to the donor-acceptor behavior between Cb and Cz, also caused the larger energy gap (from 3.91 to 4.44 eV) between the HOMO and LUMO level (Yin et al., 2018).

CONCLUSION

In summary, two carbazole-based fluorophores have been synthesized, and their photo- and electrochemical behavior has been investigated. In THF solution, carbazole based fluorophore **1** exhibits intense blue fluorescence whereas the fluorescence of carbazole/carborane based fluorophore **2** is nearly quenched completely. However, **2** exerts much stronger fluorescence emission than **1** in solid state, and exhibits aggregational induced emission enhancement behavior. Crystallographic study confirmed the tightly packing style in the condensed state of **2**. Moreover, electrochemical experiments and DFT calculations were performed to explain the donor-acceptor behavior of the carbazole based fluorophores.

EXPERIMENTAL SECTION

General Experimental Conditions

All manipulations were performed under nitrogen atmosphere by using standard Schlenk techniques unless otherwise indicated.

Chemical reagents except solvents were purchased via commercial sources and used without further purification. Tetrahydrofuran (THF) and toluene were refluxed on sodium-benzophenone system and freshly distilled prior to use. Triethylamine (Et₃N) was refluxed on CaH₂ and freshly distilled prior to use. ¹H NMR spectra were recorded on Bruker AVANCE NEO 400 MHz, ¹¹B, and ¹³C NMR spectra were recorded on Bruker AVANCE III HD 600 MHz, and CDCl₃ were used as deuterated reagent unless otherwise specified. FT-IR spectra were recorded on BIO-RAD FTS-40. Solution fluorescence spectra were recorded on PerkinElmer Fluorescence Spectrometer LS55. Solid fluorescence spectra were recorded on Edinburgh Instrument FLS980. 3,6-dibromo-9-butylcarbazole was synthesized according to reported literature (Zhu et al., 2016).

Synthesis of 9-Butyl-3,6-bis(Phenylethynyl)-9H-Carbazole (**1**)

3,6-dibromo-9-butylcarbazole (381.0 mg, 1.0 mmol), Pd(PPh₃)₄ (115.0 mg, 0.1 mmol), and CuI (20.0 mg, 0.1 mmol) were added to a Schlenk tube under inert atmosphere, and anhydrous THF (15 mL) and Et₃N (15 mL) were injected into the system. The reaction mixture was stirred at ambient temperature for 10 min, then Phenylacetylene (245.0 mg, 2.4 mmol) was injected into the mixture and stirred overnight at 90°C. After the reaction was complete according to TLC monitoring, the reaction mixture was filtered through a thin layer of silica gel to afford a lucid solution. After the solvents were removed under vacuum, the black viscous residue was diluted by CH₂Cl₂ and then washed with water and brine. The organic layers were collected and solvent was removed under reduced pressure, the crude product was subjected to chromatography column using n-hexane/ethyl acetate (v/v = 10/1) as elute to afford **1** as a yellow powder (173.4 mg, 41%). ¹H NMR (400 MHz, *d*₆-DMSO) δ(ppm): 8.50 (d, *J* = 1.0 Hz, 2H), 7.72–7.65 (m, 4H), 7.59–7.57 (dd, *J* = 8.4, 1.0 Hz, 4H), 7.47–7.41 (m, 6H), 4.45 (t, *J* = 7.1 Hz, 2H), 1.77 (p, *J* = 7.2 Hz, 2H), 1.32 (h, *J* = 7.6 Hz, 2H), 0.90 (t, *J* = 7.3 Hz, 3H).

Synthesis of 9-Butyl-3,6-Bis(2-Phenyl-*o*-Carborane)-9H-Carbazole (**2**)

Decaborane (104.0 mg, 0.85 mmol) was dissolved in CH₃CN (1.0 mL) under inert atmosphere, and then was stirred for 1 h at 60°C. After cooling to room temperature, **1** (105.0 mg, 0.25 mmol), AgNO₃ (7.0 mg, 0.04 mmol) and dry toluene (20.0 mL) were added into the reaction system, and then refluxed for 2 days. After cooling, solvents were removed under vacuum, and the black residue was subject to silica gel chromatography using n-hexane as eluent to afford **2** as a yellow powder (37.9 mg, 23%) (Toppino et al., 2013). A yellow single crystal can be obtained by recrystallization from CHCl₃ and n-hexane as combined solvents. ¹H NMR (400 MHz, CDCl₃) δ(ppm): 8.05 (d, *J* = 1.8 Hz, 2H), 7.49 (dd, *J* = 8.9, 2.2 Hz, 6H), 7.18–7.04 (m, 8H), 4.05 (t, *J* = 7.2 Hz, 2H), 3.40–1.83 (w, 20H), 1.66 (p, *J* = 7.3 Hz, 2H), 1.25–1.19 (m, 2H), 0.87 (t, *J* = 7.3 Hz, 3H). ¹³C (600 MHz, CDCl₃) δ(ppm): 159.3,

140.3, 132.9, 129.6, 124.0, 122.5, 116.0, 114.1, 114.0, 109.0, 89.2, 87.7, 55.3, 43.1, 31.1, 20.5, 13.9. ^{11}B NMR (600 MHz, CDCl_3) δ (ppm): -3.1 (4B), -11.2 (6B). IR (KBr): (ν cm^{-1}) 2,576 (B-H).

Cyclic Voltammograms Condition

CV tests were carried out with a CHI760B electrochemical workstation in CH_2Cl_2 containing 0.1 M of sample and 0.1 M of Bu_4NClO_4 at scan rate of 100 mV/s^{-1} under a nitrogen atmosphere. A three-electrodes cell system was used, containing a glassy carbon working electrode, a platinum counter electrode and an Ag/AgCl reference electrode, respectively.

Density Functional Calculations

The frontier molecular orbitals of the compounds were performed with the Gaussian 09W. Structural optimization was performed before the calculation of the HOMO/LUMO energies. The Becke3LYP(B3LYP) functional with the 6-311G(d, p) basis set was used for all calculations (Frisch et al., 2009).

X-ray Structure Determination

X-ray diffraction data was collected on a Burker Smart CCD Apex DUO diffractometer with a graphite mono-chromated $\text{CuK}\alpha$ radiation ($\lambda = 1.54184 \text{ \AA}$) using the ω - 2θ scan mode. The data were corrected for Lorenz and polarization effects. The structure was solved by direct methods and refined on F^2 by full-matrix least-squares methods using SHELXTL-2000. All calculations and molecular graphics were carried out on a computer using the SHELX-2000 program package and Diamond software.

REFERENCES

- Beverina, L., and Pagani, G. A. (2014). π -Conjugated zwitterions as paradigm of donor-acceptor building blocks in organic-based materials. *Acc. Chem. Res.* 47, 319–329. doi: 10.1021/ar4000967
- Blouin, N., and Leclerc, M. (2008). Poly(2,7-carbazole)s: structure-property relationships. *Acc. Chem. Res.* 41, 1110–1119. doi: 10.1021/ar800057k
- Chen, Z., Ono, R. J., Wiggins, K. M., Cui, H. L., Rong, C. R., Bielawski, C. W., et al. (2011). Synthesis and characterization of polyketones containing pendant carbazoles. *Polymer* 52, 1731–1737. doi: 10.1016/j.polymer.2011.02.030
- Cheng, Y. J., Yang, S. H., and Hsu, C. S. (2009). Synthesis of conjugated polymers for organic solar cell applications. *Chem. Rev.* 209, 5868–5923. doi: 10.1021/cr900182s
- Cho, Y. J., Kim, S. Y., Cho, M. J., Han, W. S., Son, H. J., Cho, D. W., et al. (2016). Aggregation-induced emission of diarylamino-pi-carborane triads: effects of charge transfer and pi-conjugation. *Phys. Chem. Chem. Phys.* 18, 9702–9708. doi: 10.1039/C5CP07883K
- Ding, D., Li, K., Liu, B., and Tang, B. Z. (2013). Bioprobes based on AIE fluorogens. *Acc. Chem. Res.* 46, 2441–2453. doi: 10.1021/ar3003464
- Frisch, M. J., Trucks, G. W., Schlegel, H. B., Scuseria, G. E., Robb, M. A., Cheeseman, J. R., et al. (2009). *Gaussian 09W (Revision A.01)*. Wallingford CT: Gaussian Inc.
- Furue, R., Nishimoto, T., Park, I. S., Lee, J. Y., and Yasuda, T. (2016). Aggregation-induced delayed fluorescence based on donor/acceptor-tethered janus carborane triads: unique photophysical properties of nondoped OLEDs. *Angew. Chem. Int. Ed Engl.* 55, 7171–7175. doi: 10.1002/anie.201603232
- Gong, W. L., Wang, B., Aldred, M. P., Li, C., Zhang, G. F., Chen, T., et al. (2014). Tetraphenylethene-decorated carbazoles: synthesis, aggregation-induced emission, photo-oxidation and electroluminescence. *J. Mater. Chem. C* 2, 7001–7012. doi: 10.1039/C4TC01019A

DATA AVAILABILITY STATEMENT

All datasets generated for this study are included in the article/Supplementary Material.

AUTHOR CONTRIBUTIONS

JJ performed the design, synthesis experiments, and collection of the data. J-XK and HL made contributions on DFT calculation. YM, QZ, and JZ made contribution on single crystal data interpretation. XC made substantial contribution on data analysis and manuscript writing.

FUNDING

Authors are grateful for the financial support from the National Natural Science Foundation of China (Grant Nos. U1804253, 2160105, and 21771057) and the 111 Project (Grant No. D17007), Henan Center for Outstanding Overseas Scientists (Grant No. GZS2018003). JJ acknowledges Henan Normal University for postdoctoral support.

SUPPLEMENTARY MATERIAL

The Supplementary Material for this article can be found online at: <https://www.frontiersin.org/articles/10.3389/fchem.2019.00768/full#supplementary-material>

- Grazulevicius, J. V., Storhriegel, P., Pielichowski, J., and Pielichowski, K. (2003). Carbazole-containing polymers: synthesis, properties and applications. *Prog. Polym. Sci.* 28, 1297–1353. doi: 10.1016/S0079-6700(03)00036-4
- Grigalevicius, S. (2006). 3,6(2,7),9-Substituted carbazoles as electroactive amorphous materials for optoelectronics. *Synth. Met.* 156, 1–12. doi: 10.1016/j.synthmet.2005.10.004
- Grimdale, A. C., Chan, K. L., Martin, R. E., Jokisz, P. G., and Holmes, A. B. (2009). Synthesis of light-emitting conjugated polymers for applications in electroluminescent devices. *Chem. Rev.* 109, 897–1091. doi: 10.1021/cr000013v
- Gunes, S., Neugebauer, H., and Sariciftci, N. S. (2007). Conjugated polymer-based organic solar cells. *Chem. Rev.* 107, 1324–1338. doi: 10.1021/cr050149z
- Guo, J. X., Liu, D. Q., Zhang, J. H., Zhang, J. J., Miao, Q., and Xie, Z. W. (2015). o-Carborane functionalized pentacenes: synthesis, molecular packing and ambipolar organic thin-film transistors. *Chem. Commun.* 51, 12004–12007. doi: 10.1039/C5CC03608A
- He, Z. K., Shan, L., Mei, J., Wang, H., Lam, J. W. Y., Sung, H. H. Y., et al. (2015). Aggregation-induced emission and aggregation-promoted photochromism of bis(diphenylmethylene)dihydroacenes. *Chem. Sci.* 6, 3538–3543. doi: 10.1039/C5SC00900F
- Hong, Y. N., Lam, J. W. Y., and Tang, B. Z. (2009). Aggregation-induced emission: phenomenon, mechanism and applications. *Chem. Commun.* 4332–4353. doi: 10.1039/b904665h
- Hong, Y. N., Lam, J. W. Y., and Tang, B. Z. (2011). Aggregation-induced emission. *Chem. Soc. Rev.* 40, 5361–5388. doi: 10.1039/c1cs15113d
- Hosoi, K., Inagi, S., Kubo, T., and Fuchigami, T. (2011). o-Carborane as an electron-transfer mediator in electrocatalytic reduction. *Chem. Comm.* 47, 8632–8634. doi: 10.1039/c1cc12912k
- Karpicz, R., Kirkus, M., Grazulevicius, J. V., and Gulbinas, V. (2010). Fluorescence quenching by charge carriers in indolo[3,2-b]carbazole-based polymer. *J. Lumin.* 130, 722–727. doi: 10.1016/j.jlumin.2009.11.029

- Kivala, M., and Diederich, F. (2009). Acetylene-derived strong organic acceptors for planar and nonplanar push-pull chromophores. *Acc. Chem. Res.* 42, 235–248. doi: 10.1021/ar8001238
- Kokado, K., and Chujo, Y. (2009). Emission via aggregation of alternating polymers with o-carborane and p-phenylene-ethynylene sequences. *Macromolecules* 42, 1418–1420. doi: 10.1021/ma8027358
- Kokado, K., Nagai, A., and Chujo, Y. (2010). Poly(γ -glutamic acid) hydrogels with water-sensitive luminescence derived from aggregation-induced emission of o-carborane. *Macromolecules* 43, 6463–6468. doi: 10.1021/ma100792z
- Kundu, P., Tomas, K. R. J., Lin, J. T., Tao, Y. T., and Chien, C. H. (2003). High-Tg carbazole derivatives as blue-emitting hole-transporting materials for electroluminescent devices. *Adv. Funct. Mater.* 13, 445–452. doi: 10.1002/adfm.200304308
- Kwon, S. N., Wee, K. R., Cho, Y. J., and Kang, S. O. (2014). Carborane dyads for photoinduced electron transfer: photophysical studies on carbazole and phenyl-o-carborane molecular assemblies. *Chemistry* 20, 5953–5960. doi: 10.1002/chem.201304474
- Li, M. J., Peng, F., Ying, L., and Xu, J. K. (2019). Sky-blue fluorescent small-molecules with high quantum efficiency: synthesis, structures, AIE properties, and applications in solution-processed non-doped OLEDs. *J. Mater. Chem. C* 7, 3553–3559. doi: 10.1039/C9TC00546C
- Li, X., Yan, H., and Zhao, Q. (2016). Carboranes as a tool to tune phosphorescence. *Chem. Eur. J.* 22, 1888–1898. doi: 10.1002/chem.201503456
- Li, Z., Lu, J., Li, S. D., Qin, S. H., and Qin, Y. M. (2012). Orderly ultrathin films based on perylene/poly(N-vinyl carbazole) assembled with layered double hydroxide nanosheets: 2D fluorescence resonance energy transfer and reversible fluorescence response for volatile organic compounds. *Adv. Mater.* 24, 6053–6057. doi: 10.1002/adma.201203040
- Liu, Y., Chen, S. M., Lam, J. W. Y., Lu, P., Kwok, R. T. K., Mahtab, F., et al. (2011). Tuning the electronic nature of aggregation-induced emission luminogens with enhanced hole-transporting property. *Chem. Mater.* 23, 2536–2544. doi: 10.1021/cm2003269
- Luo, J. D., Xie, Z., Lam, J. W., Cheng, H., Qiu, C., Kwok, H. S., et al. (2001). Aggregation-induced emission of 1-methyl-1,2,3,4,5-pentaphenylsilole. *Chem. Commun.* 2001, 1740–1741. doi: 10.1039/b105159h
- Meier, M., Ji, L., Nitsch, J., Krummenacher, I., Deißberger, A., Auerhammer, D., et al. (2019). Preparation and characterization of a pi-conjugated donor-acceptor system containing the strongly electron-accepting tetraphenylborolyl unit. *Chemistry* 25, 4707–4712. doi: 10.1002/chem.201805454
- Metzger, R. M. (1999). Electrical rectification by a molecule: the advent of unimolecular electronic devices. *Acc. Chem. Res.* 32, 950–957. doi: 10.1021/ar9900663
- Mishra, A., and Bauerle, P. (2012). Small molecule organic semiconductors on the move: promises for future solar energy technology. *Angew. Chem. Int. Ed Engl.* 51, 2020–2067. doi: 10.1002/anie.201102326
- Naito, H., Morisaki, Y., and Chujo, Y. (2015). o-Carborane-based anthracene: a variety of emission behaviors. *Angew. Chem. Int. Ed Engl.* 54, 5084–5087. doi: 10.1002/anie.201500129
- Naito, H., Nishino, K., Morisaki, Y., Tanaka, K., and Chujo, Y. (2017). Highly-efficient solid-state emissions of anthracene-o-carborane dyads with various substituents and their thermochromic luminescence properties. *J. Mater. Chem. C* 5, 10047–10054. doi: 10.1039/C7TC02682J
- Naito, H., Uemura, K., Morisaki, Y., Tanaka, K., and Chujo, Y. (2018). Enhancement of luminescence efficiencies by thermal rearrangement from ortho- to meta-carborane in bis-carborane-substituted acenes. *Eur. J. Org. Chem.* 2018, 1885–1890. doi: 10.1002/ejoc.201800151
- Nghia, N. V., Jana, S., Sujith, S., Ryu, J. Y., Lee, J., Lee, S. U., et al. (2018b). Nido-carboranes: donors for thermally activated delayed fluorescence. *Angew. Chem. Int. Ed Engl.* 57, 12483–12488. doi: 10.1002/anie.201806922
- Nghia, N. V., Oh, J. H., Sujith, S., Jung, J. H., and Lee, M. H. (2018a). Tuning the photophysical properties of carboranyl luminophores by closo- to nido-carborane conversion and application to OFF-ON fluoride sensing. *Dalton Transac.* 47, 17441–17449. doi: 10.1039/C8DT03771J
- Nishimoto, T., Yasuda, T., Lee, S. Y., Kondo, R., and Adachi, C. (2014). A six-carbazole-decorated cyclophosphazene as a host with high triplet energy to realize efficient delayed-fluorescence OLEDs. *Mater. Horiz.* 1, 264–269. doi: 10.1039/C3MH00079F
- Nishino, K., Hashimoto, K., Tanaka, K., Morisaki, Y., and Chujo, Y. (2016). Synthesis and properties of highly-rigid conjugation system based on bi(benzo[b]thiophene)-fused o-carborane. *Tetrahedron Lett.* 57, 2025–2028. doi: 10.1016/j.tetlet.2016.03.069
- Nishino, K., Uemura, K., Gon, M., Tanaka, K., and Chujo, Y. (2017). Enhancement of aggregation-induced emission by introducing multiple o-carborane substitutions into triphenylamine. *Molecules* 22:E2009. doi: 10.3390/molecules22112009
- Núñez, R., Tarres, M., Ferrer-Ugalde, A., Fabrizi de Biani, F., and Teixidor, F. (2016). Electrochemistry and photoluminescence of icosahedral carboranes, boranes, metallocarboranes, and their derivatives. *Chem. Rev.* 116, 14307–14378. doi: 10.1021/acs.chemrev.6b00198
- Ooyama, Y., Yamaguchi, N., Inoue, S., Nagano, T., Miyazaki, E., Fukuoka, H., et al. (2012). Mechanofluorochromism of carbazole-type D- π -A fluorescent dyes. *Tetrahedron* 68, 529–533. doi: 10.1016/j.tet.2011.11.012
- Toppino, A., Genady, A. R., El-Zaria, M. E., Reeve, J., Mostofian, F., Kent, J., et al. (2013). High yielding preparation of dicarba-closo-dodecaboranes using a silver(I) mediated dehydrogenative alkyne-insertion reaction. *Inorg. Chem.* 52, 8743–8749. doi: 10.1021/ic400928v
- Uoyama, H., Goushi, K., Shizu, K., Nomura, H., and Adachi, C. (2012). Highly efficient organic light-emitting diodes from delayed fluorescence. *Nature* 492, 234–238. doi: 10.1038/nature11687
- Wang, Z. Y., Feng, Y. Q., Wang, N. N., Cheng, Y. X., Quan, Y. W., and Ju, H. X. (2018). Donor-acceptor conjugated polymer dots for tunable electrochemiluminescence activated by aggregation-induced emission-active moieties. *J. Phys. Chem. Lett.* 9, 5296–5302. doi: 10.1021/acs.jpcl.8b02087
- Wee, K. R., Cho, Y. J., Jeong, S. Y., Kwon, S. N., Lee, J. D., Suh, I. H., et al. (2012b). Carborane-based optoelectronically active organic molecules: wide band gap host materials for blue phosphorescence. *J. Am. Chem. Soc.* 134, 17982–17990. doi: 10.1021/ja3066623
- Wee, K. R., Cho, Y. J., Song, J. K., and Kang, S. O. (2013). Multiple photoluminescence from 1,2-dinaphthyl-ortho-carborane. *Angew. Chem. Int. Ed Engl.* 52, 9682–9685. doi: 10.1002/anie.201304321
- Wee, K. R., Han, W. S., Cho, D. W., Kwon, S. N., Pac, C. J., and Kang, S. O. (2012a). Carborane photochemistry triggered by aryl substitution: carborane-based dyads with phenyl carbazoles. *Angew. Chem. Int. Ed Engl.* 51, 2677–2680. doi: 10.1002/anie.201109069
- Wei, X., Zhu, M. J., Cheng, Z., Lee, M. J., Yan, H., Lu, C. S., et al. (2019). Aggregation-induced electrochemiluminescence of carboranyl carbazoles in aqueous media. *Angew. Chem. Int. Ed Engl.* 58, 3162–3166. doi: 10.1002/anie.201900283
- Wex B., and Kaafarani, B. R. (2017). Perspective on carbazole-based organic compounds as emitters and hosts in TADF applications. *J. Mater. Chem. C* 5, 8622–8653. doi: 10.1039/C7TC02156A
- Wu, Q. J., Wang, M. H., Cao, X. D., Zhang, D., Sun, N., Wan, S. G., et al. (2018). Carbazole/ α -carboline hybrid bipolar compounds as electron acceptors in exciplex or non-exciplex mixed cohosts and exciplex-TADF emitters for high-efficiency OLEDs. *J. Mater. Chem. C* 6, 8784–8792. doi: 10.1039/C8TC02353K
- Wu, X. Y., Guo, J. X., Quan, Y. J., Jia, W., Jia, D. Z., Chen, Y., et al. (2018). Cage carbon-substitute does matter for aggregation-induced emission features of o-carborane-functionalized anthracene triads. *J. Mater. Chem. C* 6, 4140–4149. doi: 10.1039/C8TC00380G
- Xiao, L. X., Chen, Z. J., Xu, B., Luo, J. X., Kong, S., Gong, Q. H., et al. (2011). Recent progresses on materials for electrophosphorescent organic light-emitting devices. *Adv. Mater.* 23, 926–952. doi: 10.1002/adma.201003128
- Yang, L. L., Wang, J. P., Yang, L., Zhang, C., Zhang, R. L., Zhang, Z. P., et al. (2016). Fluorescent paper sensor fabricated by carbazole-based probes for dual visual detection of Cu²⁺ and gaseous H₂S. *RSC Adv.* 6, 56384–56391. doi: 10.1039/C6RA10293J
- Yin, Y. H., Li, X., Yan, S. B., Yan, H., and Lu, C. S. (2018). Tetraphenylethylene-carborane-tetraphenylethylene triad: influence of steric bridge on aggregation-induced emission properties. *Chem. Asian J.* 13, 3155–3159. doi: 10.1002/asia.201801172
- Yokoyama, M., Inada, K., Tsuchiya, Y., Nakanotani, H., and Adachi, C. (2018). Trifluoromethane modification of thermally activated delayed fluorescence

- molecules for high-efficiency blue organic light-emitting diodes. *Chem. Commun.* 54, 8261–8264. doi: 10.1039/C8CC03425G
- Zhang, J., Xu, W., Sheng, P., Zhao, G. Y., and Zhu, D. B. (2017). Organic donor-acceptor complexes as novel organic semiconductors. *Acc. Chem. Res.* 50, 1654–1662. doi: 10.1021/acs.accounts.7b00124
- Zhu, H. T., Shi, B. B., Chen, K. X., Wei, P. F., Xia, D. Y., Mondal, J. H., et al. (2016). Cyclo[4]carbazole, an iodide anion macrocyclic receptor. *Org. Lett.* 18, 5054–5057. doi: 10.1021/acs.orglett.6b02500
- Zhu, L. N., Yang, C. L., and Qin, J. G. (2008). An aggregation-induced blue shift of emission and the self-assembly of nanoparticles from a novel amphiphilic oligofluorene. *Chem. Commun.* 6303–6305. doi: 10.1039/b815431g

Conflict of Interest: The authors declare that the research was conducted in the absence of any commercial or financial relationships that could be construed as a potential conflict of interest.

Copyright © 2019 Jiao, Kang, Ma, Zhao, Li, Zhang and Chen. This is an open-access article distributed under the terms of the Creative Commons Attribution License (CC BY). The use, distribution or reproduction in other forums is permitted, provided the original author(s) and the copyright owner(s) are credited and that the original publication in this journal is cited, in accordance with accepted academic practice. No use, distribution or reproduction is permitted which does not comply with these terms.